ES Energy & Environment

DOI: https://dx.doi.org/10.30919/esee8c434

Effects of Functional Additives on Structure and Properties of Polycarbonate-Based Composites Filled with Hybrid Chopped Carbon Fiber/Graphene Nanoplatelet Fillers

Zhixing Yu*, Yu Bai, James H. Wang* and Yingcheng Li*

Abstract

A rheology modifier (styrene-acrylonitrile copolymer, SAN) and a flame retardant (resorcinol bis(2, 6-dixylyl phosphate), RXP) were incorporated in polycarbonate (PC)/chopped carbon fiber (CCF)/graphene nanoplatelet (GNP) system to prepare PC-based composites (PC/SAN$_x$@(CCF+GNP), *r*PC/SAN$_x$@(CCF+GNP)$_i$) by a twin-screw extruder. The rheological properties, thermal stability, flame retardancy and mechanical properties of composites were evaluated. Increasing shear rate and temperature induced obvious reduction of viscosity of all composites. By comparison, PC/SAN$_5$@(CCF+GNP) possessed a greater viscous flow activation energy (Eη), showing higher temperature sensibility of viscosity. While PC/SAN$_0$@(CCF+GNP) and *r*PC/SAN$_5$@(CCF+GNP)$_{1.5}$ had lower Eη values and exhibited different sensitivity of shearing force. Besides, SAN and RXP had obvious influences on the thermal stability of composites. Meanwhile, PC/SAN composites displayed improved flame retardancy from 31.9% of limiting oxygen index (LOI) and V-1 rating for PC/SAN composites to 37.9% of LOI and V-0 rating for composites containing 2.5% RXP. Additionally, mechanical strengths and moduli of PC/SAN composites were increased by SAN and RXP without impairing toughness. These results were attributed to matrix enhancement of SAN, the lubrication effect of lower molecular weight RXP and the enhancement of the interactions between matrix and fillers.

Keywords: Polycarbonate composite; Rheology; Thermal stability; Flame retardancy; Mechanical property.
Received: 14 January 2021; Accepted date: 14 March 2021.
Article type: Research article.

1. Introduction

Carbon materials, consisting of carbon fiber, carbon nanotube, graphite, graphene, *etc*, usually possess a wide range of aspect ratios, high surface to volume ratio, superior thermal conductivity, unique structure, good thermal and physicochemical stability.[1-5] Recently, carbon materials were applied in polymer material modifications, and carbon materials reinforced thermoplastic or thermosetting resins have been extensively developed to utilize their low thermal expansion, light-weighting, good heat dissipation and high stiffness.[6-11] Potential applications contain integrated circuits, satellite devices, thermal management fields, electrnonics packaging and encapsulation, etc.

Polycarbonate (PC) is one of the most important engineering plastics, and it is broadly applied in electric and electronic fields because it has good processability, high heat distortion temperature, good mechanical properties and excellent chemical resistance. PC-based thermoplastic composites filled with different carbon materials, such as multi-walled carbon nanotube, carbon fiber, expanded or flake graphite, grapheme, etc. have been studied.[12-25] However, they usually show low impact strength and brittle behaviors.[26, 27] In our previous study, factors dominating the thermal and mechanical properties including different tougheners, chopped carbon fiber (CCF)/graphene nanoplatelet (GNP) component, fiber length, surface-coated CCF of composites were investigated to enhance the toughness and thermal conductivity of PC-based composites.[28,29] Besides, a molecular dynamics approach was proposed by Sharma *et al* to characterize the thermo-mechanical properties of multi-walled carbon nanotube reinforced PC composites.[30]

On the other hand, due to the continuously growing market segment of electronic engineering products, the flame retardancy of PC or PC-based composites is becoming of increasing interest. Halogen-free flame retardants based on phosphorous, silicon and nitrogen compounds have been well developed. Environment-friendly aryl phosphate flame

R&D Division for Synthetic Polymers, Sinopec Shanghai Research Institute of Petrochemical Technology, Shanghai 201208, China.
**E-mail:* yvzx.sshy@sinopec.com (Z. Yu);
JamesWang.sshy@sinopec.com (J. H. Wang);
liyc.sshy@sinopec.com (Y. Li)

retardants, such as triphenyl phosphate (TPP), resorcinol bis(disphenyl phosphate) (RDP), bisphenol A bis(diphenylphosphate) (BDP), tetra-2,6-dimethyl phenyl resorcinol diphosphate (DMP-RDP), biphenyl bis(diphenyl phosphate) (BBDP),[31-34] are effective in improving the flame retardancy of PC alloys. Furthermore, rheometers such as modular compact rheometer or capillary rheometer have been extensively applied to study the linear or non-linear viscoelastic rheological properties of polymeric melts and solutions for many years.[35-38] In this work, the effects of rheology modifier (SAN) and flame retardant (RXP) on the structures and rheology, and mechanical performances of PC-based composites were investigated. The flammability was evaluated by UL-94 and limiting oxygen index tests. Besides, the rheological behaviors of composites were investigated by modular impact rheometer.

2. Experimental

2.1 Materials

Commercial PC with melt flow rate (MFR) of 12.3 g (10 min^{-1}) was supplied by Mitsubishi Engineering Plastics Co., Japan. SAN (25 wt% of acrylonitrile) with a number average molecular weight of 34000 g mol^{-1} and a polydispersity of 1.73 was obtained from Nantong RZS New Technology Co., China. CCFs coated by a polyethylene terephthalate (PET) layer with an average diameter of 16 μm and an average length of 6 mm were purchased from Shanghai Kajet Chemicals and Technology Co., China. GNPs with an average diameter of 150 μm and an average thickness of 100 nm were purchased from Qingdao Yanhai Carbon Materials Co., China. RXP was purchased from Shouguang OLS Chemicals Co., China. 3-aminopropyl triethoxy silane (ATS) was obtained from Sinopharm Chemical Reagent Co., China. White oil was purchased from Nanjing HongHan Petrochemistry Co., China. Antioxidant (Irganox 1010) was purchased from Shanghai Ciba Specialty Chemicals Co., China. All additives were used as received without further purification.

2.2 Preparation of PC-based composites

Four PC-based composites and three flame retardant PC-based composites were prepared according to the method expressed in Ref. 28, and their compositions were summarized in Table 1. The materials were pre-mixed at room temperature, and then the mixtures were compounded on a twin-screw extruder (MICRO 27/GL, Leistritz, German) at a temperature of 280 °C and a rotation speed of 150 rpm with a throughput of 5 kg h^{-1}. In PC/SAN$_x$@(CCF+GNP), x expresses the mass fraction of SAN, and in rPC/SAN$_x$@(CCF+GNP)$_i$, r means flame retardance, and i denotes the mass fraction of RXP. The mass fractions of SAN were set at 0, 3, 5 and 8%, and the usages of RXP were 0, 0.5, 1.5 and 2.5%, respectively. All blends included 1.00% of white oil, 0.05% of ATS and 0.80% of Irganox 1010. The samples for mechanical property and flame retardancy measurements were prepared by injection molding (M55, BOY, German) at a melt temperature of 280 °C and a mold temperature of 60 °C.

3.Characterization

3.1 Rheological properties

The rheological behavior and different rheological parameters were examined by a MCR 302 modular compact rheometer (Anton Paar, Austria). All tests were conducted on parallel plate with a gap of 0.50 mm under nitrogen atmosphere to avoid oxidative degradation. The measurement temperatures were set on 280~310 °C, and the applied shear rates were in the range of 0.1~100 s^{-1}.

3.2 Thermal properties

MFR was measured according to ISO 1133 by a 50 M melt flow indexer (Instron-CEAST, USA) under 1.2 kg loading and at 300 °C. Thermogravimetric analysis (TGA) was carried out using a Discovery thermogravimetric analyzer (TA Instruments, USA). Samples were measured in an alumina crucible with a mass of about 10 mg from 40°C to 700 °C at a heating rate of 10 °C min^{-1} under air atmosphere.

3.3 Flame retardance

Limited oxygen index (LOI) was measured using a F101 limited oxygen index meter (Shanghai Qinsun Instruments Co., China) according to ISO 4589.2 standard. The specimen dimension was 80 mm × 10 mm × 4 mm. UL94 vertical burning test was performed using a AN6150A horizontal vertical flame tester (Shenzhen Angui Instrument Co., China) according to ASTM D3801-2010. The dimensions of samples were 127 mm × 12.7 mm × 3.2 mm.

3.4 Mechanical properties

Notched Charpy impact tests were carried out according to ISO 179 using a RESIL6957 impact tester (CEAST, Italy) on the standard sized rectangular bars at room temperature. The depth of nick was 2 mm. Flexural properties were characterized according to ISO 178 by a 3344 universal material machine (Instron, USA). The tests were conducted at

Table 1. Compositions of the investigated PC-based composites.

Materials	PC/SAN$_x$@(CCF+GNP)				rPC/SAN$_5$@(CCF+GNP)$_i$		
	x = 0	x = 3	x = 5	x = 8	i = 0.5	i = 1.5	i = 2.5
PC	70	67	65	62	65	65	65
SAN	0	3	5	8	5	5	5
CCF	25	25	25	25	25	25	25
GNP	5	5	5	5	5	5	5
RXP	0	0	0	0	0.5	1.5	2.5

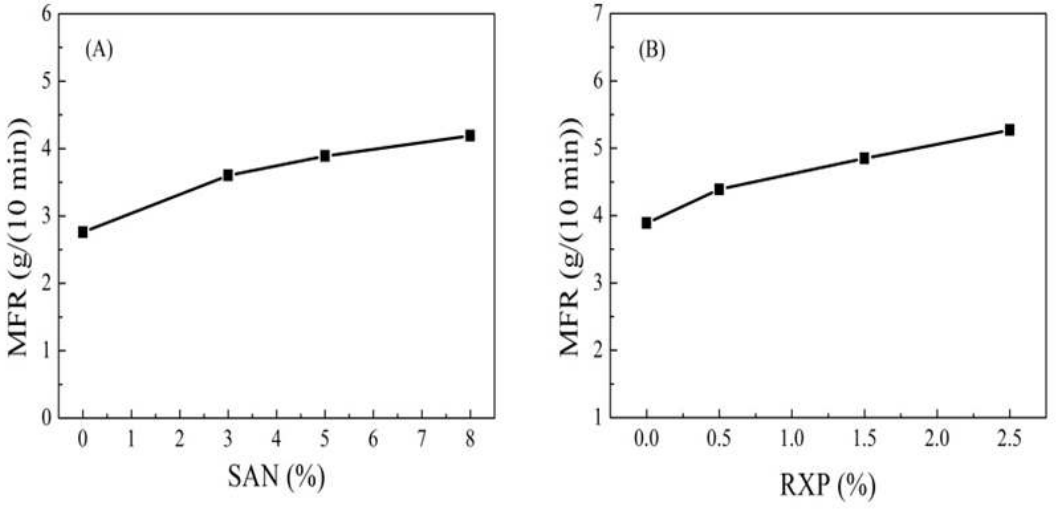

Fig. 1 Variation of melt flow rate of PC-based composites with (A) SAN and (B) RXP content.

room temperature using a bending rate of 2 mm min^{-1} and a span of 64 mm. Tensile properties were measured by ISO 527-2 standard using a 3367 universal material machine (Instron, USA). The extensometer load is 10 KN. The tests were conducted at room temperature using a cross-head rate of 50 mm min^{-1}. At least five specimens were tested for each sample to get an average value.

3.5 Morphology

The surface morphologies of char residue samples obtained from the impact fracture surfaces were observed using a merlin field-emission scanning electron microscope (FE-SEM) (ZEISS, German). The specimens were previously coated with a conductive layer of gold.

4. Results and discussion

4.1 Melt flow and rheological properties

The MFR values of PC-based composites under different SAN and RXP contents were shown in Fig. 1. As for PC/SAN_x@(CCF+GNP) composites, with the SAN content increasing, MFR gradually increased. Comparison with PC/SAN_0@(CCF+GNP) (2.76 g (10 min^{-1})), the values of PC/SAN_3@(CCF+GNP), PC/SAN_5@(CCF+GNP) and PC/SAN_8@(CCF+GNP) were 3.60, 3.89 and 4.19 g (10 min^{-1}); the relative enhancement of MFR was 30.4%, 40.9% and 51.8%, respectively. These results indicated an obvious improvement of melt fluidity and SAN being an effective fluidity improver. At the same time, the MFR values of *r*PC/SAN_5@(CCF+GNP)$_i$ also displayed an approximately linear and increasing trend with an increase in RXP content. When the RXP content was gradually increased to 2.5%, the MFR value was improved from 3.89 g (10 min^{-1}) to 5.27 g (10 min^{-1}), and the highest enhancement was 35.5%. Therefore, introducing SAN and RXP into the PC/hybrid filler system could effectively enhance the fluidity and processability of composites.

On the other hand, as the quality and performances of products were directly affected by the processing parameters, the study for the rheological behaviors of materials was instructive and significant to polymer processing. In this work, rheological properties of PC-based composites with different content of SAN and RXP were measured. Apparent viscosity as a function of shear rate was measured at 300 °C to determine the viscosity curves of composites (Fig. 2). As seen in Fig. 2A, the non-Newtonian behavior of PC/SAN_x@(CCF+GNP) composites were observed. As the shear rate increased from

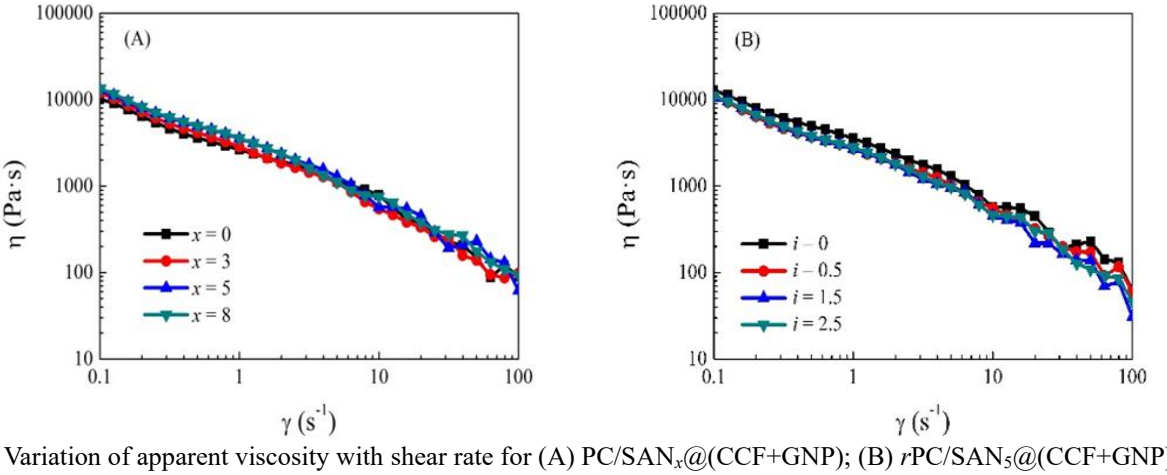

Fig. 2 Variation of apparent viscosity with shear rate for (A) PC/SAN_x@(CCF+GNP); (B) *r*PC/SAN_5@(CCF+GNP)$_i$.

0.1 s^{-1} to 100 s^{-1}, a continuous reduction of viscosity from about 10000 Pa·s to about 100 Pa·s were recorded. Moreover, with increasing SAN content, the apparent viscosity of composites increased slightly. These observations predicted that PC/SAN_x@(CCF+GNP) had more compact microstructures and well compatible system. SAN played a role in the enhancement for the polycarbonate matrix. On the other hand, the pseudo-plastic behaviors of *r*PC/SAN_5@$(CCF+GNP)_i$ as well as their variations of viscosity with shear rate were similar to the PC/SAN_x@(CCF+GNP) (Fig. 2B). Besides, the apparent viscosity of each flame retardant composite slightly decreased with the increase of RXP content. These results were attributed to the lubrication effect of RXP additive with a lower molecular weight. Therefore, the addition of SAN and RXP was beneficial to the enhancement of the interactions between matrix and fillers.

Furthermore, the viscous flow activation energy reflected not only the melt flowing property of material, but also its temperature sensitivity of viscosity change.[39] The relationship between apparent viscosity and temperature was following Arrhenius empirical formula above the viscous flow temperature. The derivative formula was given by equation (1):

$$\ln \eta = A' + \frac{E\eta}{R \cdot T} \quad (1)$$

where η was apparent viscosity, A' was a constant, Eη was viscous flow activation energy, R was gas constant, and T was absolute temperature. By fitting equation, lnη and 1/T showed a linear relationship and the slope was Eη/R.

Fig. 3 showed the variation of apparent viscosity of three typical PC-based composites (PC/SAN_0@(CCF+GNP), PC/SAN_5@(CCF+GNP) and *r*PC/SAN_5@$(CCF+GNP)_{1.5}$) with shear rate at different temperature. There were no exceptions that all curves displayed continuous reduction of viscosity with an increase of shear rate. Moreover, at a constant shear rate, a rise in the melt temperature leaded to a lower viscosity of composite. Four different shear rates were selected for determining the relationship between lnη and 1/T. The respective fitting curves and the calculated Eη values were shown in Fig. 4 and Table 2, respectively.

Within the experimental temperature range, Eη values of PC/SAN_0@(CCF+GNP) and *r*PC/SAN_5@$(CCF+GNP)_{1.5}$ decreased as the shear rate increased, indicating a reduced temperature sensitivity of viscosity of composite; while Eη values of PC/SAN_5@(CCF+GNP) increased with increase of shear rate, indicating an enhanced temperature sensitivity of viscosity of composites. Note that Eη value had no direct relationship with viscosity value. A decreased viscous flow activation energy corresponded to a degressive potential barrier for molecular motions. That could be explained by the inter-molecular un-entanglement and weakened interactions due to the external shearing actions.

The lnEη ~ lnγ relations were also fitted and the results were listed in Table 2. The resultant slope expressed the

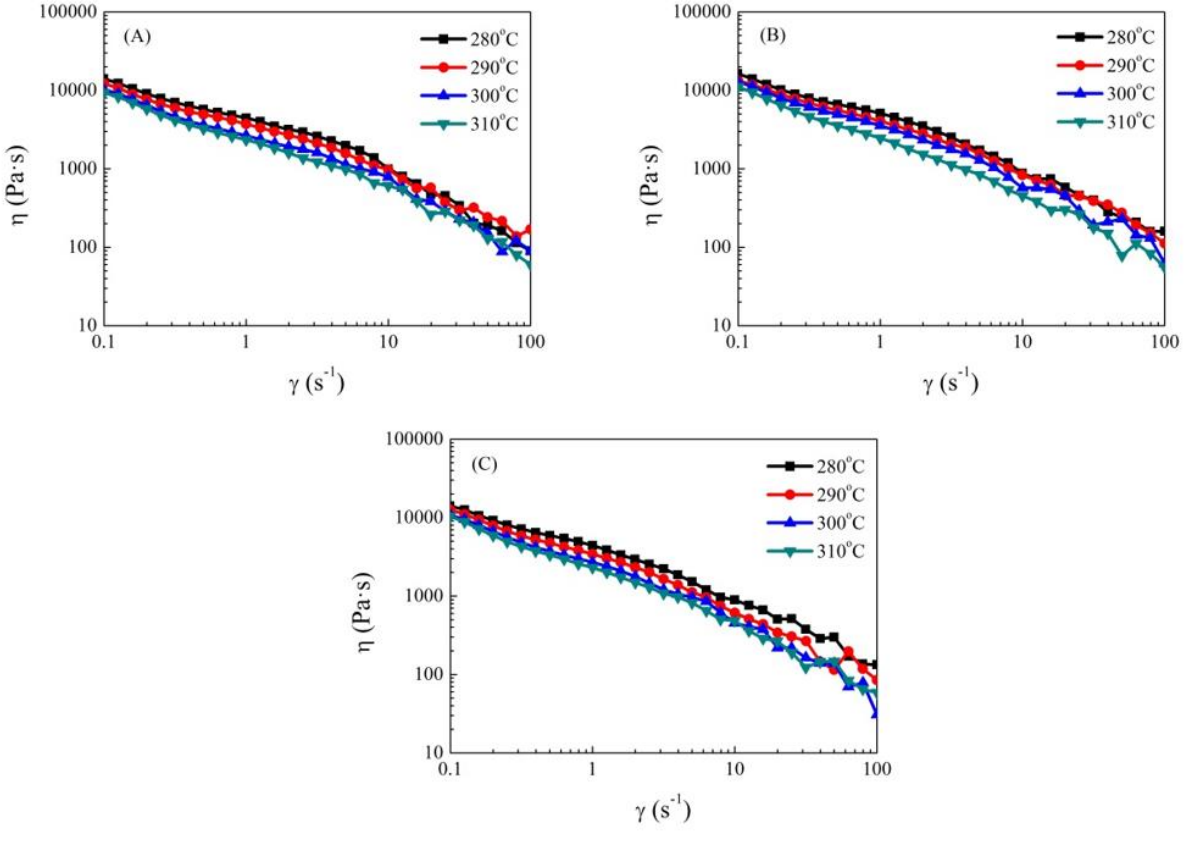

Fig. 3 Variation of apparent viscosity with shear rate under different temperature: (A) PC/SAN_0@(CCF+GNP); (B) PC/SAN_5@(CCF+GNP); (C) *r*PC/SAN_5@$(CCF+GNP)_{1.5}$.

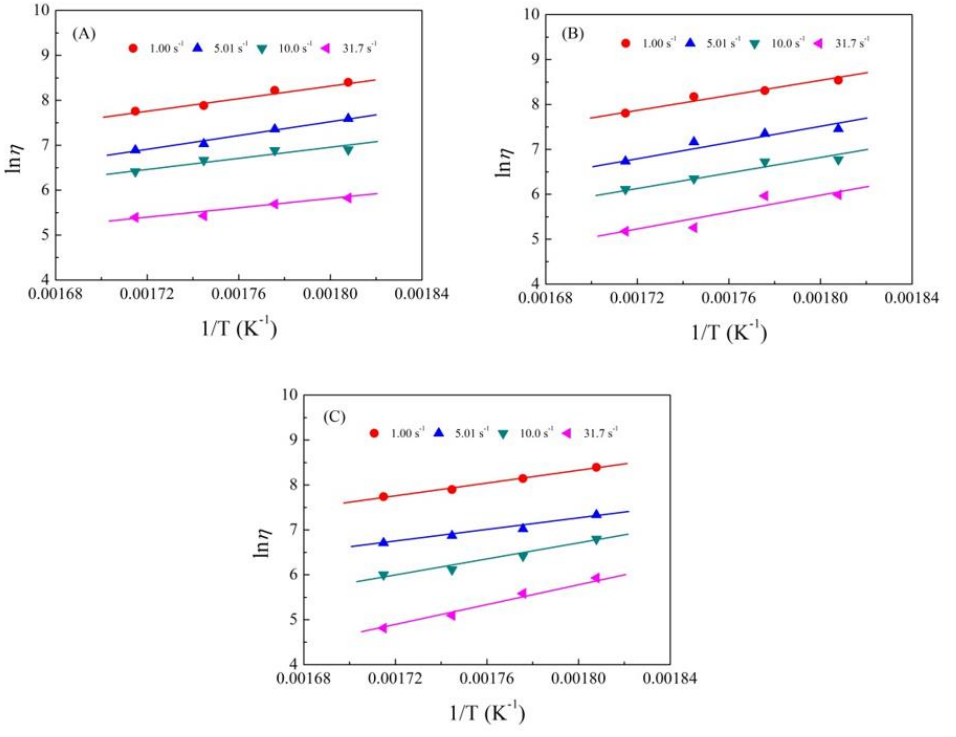

Fig. 4 lnη ~ 1/T curves for (A) PC/SAN$_0$@(CCF+GNP); (B) PC/SAN$_5$@(CCF+GNP); (C) *r*PC/SAN$_5$@(CCF+GNP)$_{1.5}$ under different shear rates.

Table 2. Viscous flow activation energies of PC-based composites.

Sample	γ (s^{-1})	lnη ~ 1/T relation	Eη (kJ mol^{-1})	lnEη ~ lnγ relation
PC/SAN$_0$@(CCF+GNP)	1.00	lnη = -4.82 + 7319 · 1/T	60.85	lnEη = 1.8152 – 0.1210 · lnγ
	5.01	lnη = -6.60 + 7846 · 1/T	65.23	
	10.0	lnη = -2.80 + 5405 · 1/T	44.94	
	31.7	lnη = -3.28 + 5036 · 1/T	41.87	
PC/SAN$_5$@(CCF+GNP)	1.00	lnη = -4.98 + 7491 · 1/T	62.28	lnEη = 1.7660 + 0.0780 · lnγ
	5.01	lnη = -6.15 + 7566 · 1/T	62.90	
	10.0	lnη = -6.88 + 7590 · 1/T	63.10	
	31.7	lnη = -12.25 + 10134 · 1/T	84.25	
*r*PC/SAN$_5$@(CCF+GNP)$_{1.5}$	1.00	lnη = -4.50 + 7124 · 1/T	59.23	lnEη = 1.7690– 0.0270 · lnγ
	5.01	lnη = -4.55 + 6551 · 1/T	54.47	
	10.0	lnη = -5.77 + 6897 · 1/T	57.34	
	31.7	lnη = -6.17 + 6398 · 1/T	53.19	

variation level of viscosity with shear rate. By comparison, PC/SAN$_5$@(CCF+GNP) possessing higher Eη value and 0.0780 of slope showed greater variation of the processing property when temperatures were fluctuated. For this case, a more precise control of temperature was needed. In other words, a rise temperature was beneficial for processability and reducing substantially the melt viscosity under this situation. As for the PC/SAN$_0$@(CCF+GNP) and *r*PC/SAN$_5$@(CCF+GNP)$_{1.5}$, the processing property could be easily improved through adjusting the shear rate. Besides, the variation level of Eη value of PC/SAN$_0$@(CCF+GNP) with shear rate was larger than that of *r*PC/SAN$_5$@(CCF+GNP)$_{1.5}$, meaning a strong sensibility of shearing force. However, since temperature evidently affected the rheological properties of *r*PC/SAN$_5$@(CCF+GNP)$_{1.5}$ in a wide shear rate range, more attention also should be paid in the process of actual production.

4.2 Thermogravimetric analysis and flame retardancy

The thermogravimetric (TG) and differential thermogravimetric (DTG) curves of PC-based composites PC/SAN*x*@(CCF+GNP) and *r*PC/SAN$_x$@(CCF+GNP)$_i$ as

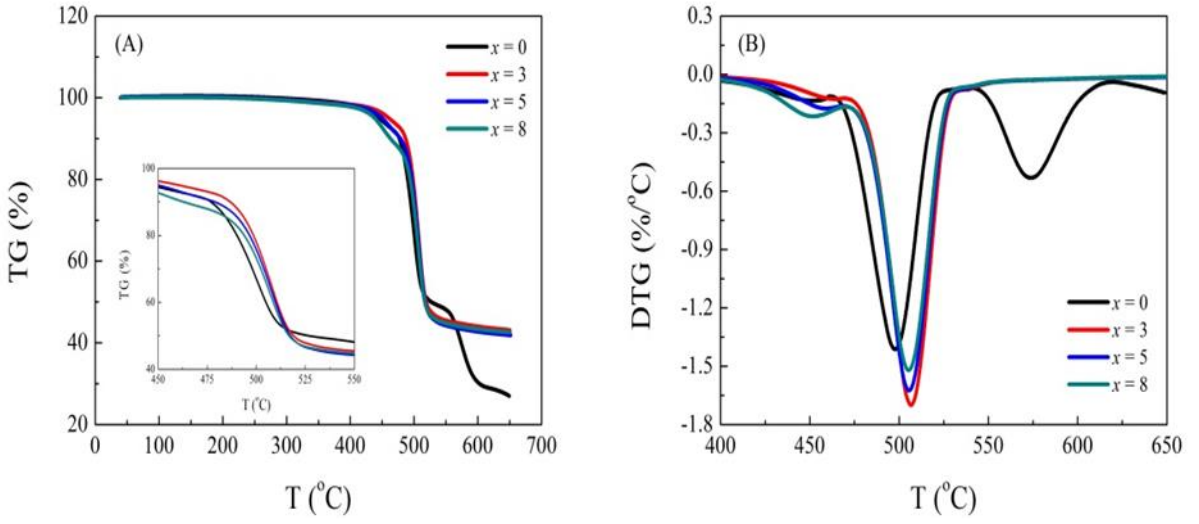

Fig. 5 (A) TG and (B) DTG curves of PC/SAN$_x$@(CCF+GNP) in air at the heating rate of 10 °C min^{-1}.

well as RXP under an air atmosphere are shown in Figs. 5 and 6, respectively. The temperatures of 5 wt% weight loss ($T_{5wt\%}$), the temperatures of the maximum weight loss rate (T_{max}), and the char residue yield at 650 °C of the samples were obtained from the curves and listed in Table 3. In this work, the PC-based composites with or without flame retardant modification were prepared by melt-extrusion method at a temperature ranging from 220 °C to 280 °C, and injection-molded at a temperature ranging from 260 °C to 280 °C. The processing temperatures were at less 40 °C lower than the onset decomposition temperature of RXP ($T_{5wt\%}$ = 321.1 °C). So the influence of the machining process on the thermal stability of PC-based composites was neglected. The $T_{5wt\%}$ value of PC/SAN$_0$@(CCF+GNP) was 445.5 °C, and it presented three temperatures of maximum weight loss rate (R_{max}): the first T_{max} of PC/SAN$_0$@(CCF+GNP) was about 454.5 °C (R_{max} = 0.14% °C^{-1}), the second T_{max} was approximately 497.8 °C (R_{max} = 1.41% °C^{-1}) and the third T_{max} was 574.0 °C (R_{max} = 0.53% °C^{-1}). When SAN was introduced to PC-based composite system, the PC/SAN$_x$@(CCF+GNP) composites also showed three separate thermal decomposition stages. Compared to PC/SAN$_0$@(CCF+GNP), the $T_{5wt\%}$, T_{max1}, T_{max2} as well as R_{max2} values obviously increased and then decreased; the R_{max1} values showed slight increase while T_{max3} and R_{max3} values decreased sharply ($\triangle T_{max3}$ = 34.5~36.3 °C and $\triangle R_{max3}$ = 0.45~0.47% °C^{-1}) and then showed no significant difference. These results indicated that SAN contributed to a relative higher thermal stability for the composite. The PC/SAN composites mainly decomposed between 430 °C and 550 °C and their residues at 650 °C were improved by 14.9~16.1% relate to the PC composite system without SAN.

As for the flame retardancy PC-based composites, the thermal decomposition processes were similar to the PC/SAN$_5$@(CCF+GNP). However, the obvious lower $T_{5wt\%}$ and T_{max1} values than those without RXP systems, reduced approximately 11.0~18.4 °C and 0.7~5.2 °C, respectively. It

Table 3. Summary for thermogravimetric results of RXP and PC-based composites under an air atmosphere.

Sample	$T_{5wt\%}$[a] (°C)	Stage I		Stage II		Stage III		Residue at 650°C (%)
		T_{max1}[b] (°C)	R_{max1}[c] (% °C^{-1})	T_{max2}[b] (°C)	R_{max2}[c] (% °C^{-1})	T_{max3}[b] (°C)	R_{max3}[c] (% °C^{-1})	
RXP	321.1	428.1	1.84	462.3	0.11	/	/	< 0.1
PC/SAN$_0$@(CCF+GNP)	445.5	451.5	0.14	497.8	1.41	574.0	0.53	27.0
PC/SAN$_3$@(CCF+GNP)	460.6	464.1	0.13	506.9	1.70	538.3	0.08	43.1
PC/SAN$_5$@(CCF+GNP)	450.0	459.4	0.18	505.7	1.62	537.7	0.07	41.9
PC/SAN$_8$@(CCF+GNP)	438.4	452.1	0.21	505.4	1.52	539.5	0.06	42.6
*r*PC/SAN$_5$@(CCF+GNP)$_{0.5}$	439.0	454.2	0.13	513.4	1.73	543.4	0.07	41.9
*r*PC/SAN$_5$@(CCF+GNP)$_{1.5}$	439.0	457.3	0.14	515.4	1.71	543.7	0.08	42.3
*r*PC/SAN$_5$@(CCF+GNP)$_{2.5}$	431.6	458.7	0.15	512.9	1.66	541.9	0.08	43.1

[a] The temperature at which 5 wt% weight loss rate occurred.

[b] The temperature at which the maximum weight loss rate occurred.

[c] The absolute values of maximum weight loss rate.

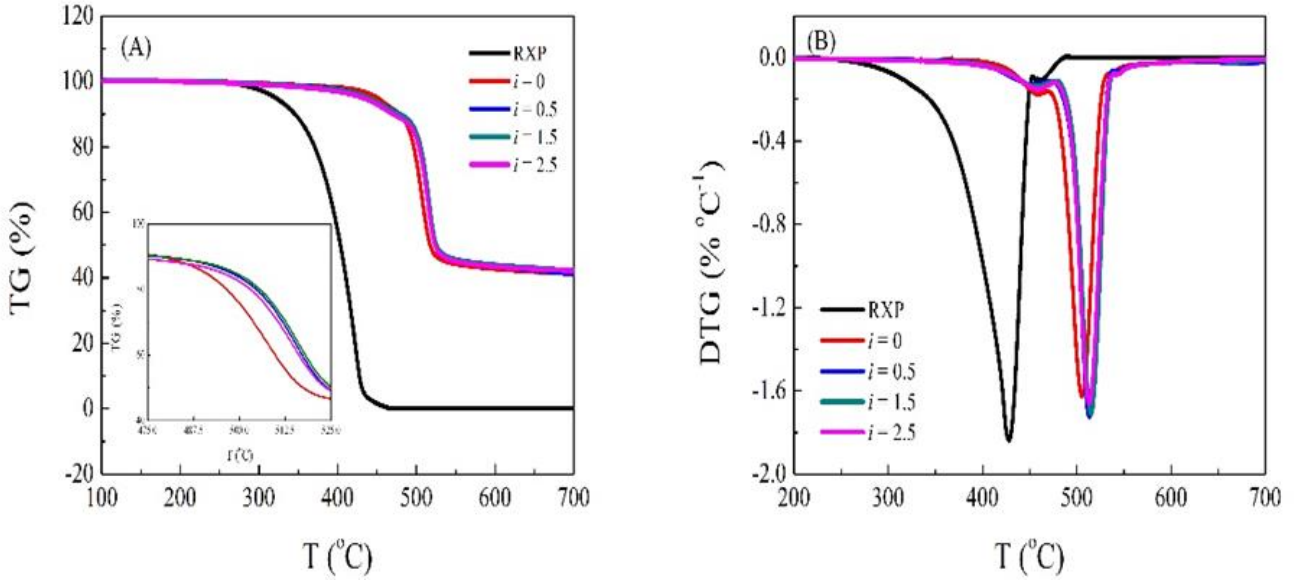

Fig. 6 (A) TG and (B) DTG curves of RXP and *r*PC/SAN$_5$@(CCF+GNP)$_i$ in air at the heating rate of 10 °C min^{-1}.

was mainly attributed to a relatively lower thermal decomposition temperature of RXP. This also indicated that the addition of RXP had a very obvious influence on the thermal stability of *r*PC/SAN$_x$@(CCF+GNP)$_i$. Besides the gradual increase of T_{max1}, higher T_{max2} and T_{max3} indicated a good thermal stability in the presence of RXP, and the excellent thermal stability was a requisite for flame retardance of material. As a consequence, further increased char residue amount was achieved. It showed that a small amount of RXP had a little influence on the char residue formation of *r*PC/SAN$_x$@(CCF+GNP)$_i$. The reason was that the produced oxyacid or anhydrous phosphoric acid covered the composite matrix. It isolated oxygen and heat diffusion, and on the other hand, it prevented formation of combustible gases or liquids.[40] In addition, it should be noted that a decrease in R_{max2} with increasing RXP amount but still higher than the sample without RXP leaded to a higher thermal decomposition temperature (>512.0 °C).

Table 4 lists the LOI values, UL94 results and flame retardance of PC-based composites with different contents of SAN and RXP. It is well known that PC and its alloys were no vertical rating, and a large amount of black and dense smoke was released during the LOI testing process.[33] The PC-based composites containing hybrid chopped carbon fiber and graphene nanoplatelet fillers displayed excellent flame retardancy and showed 31.0% of LOI and UL94 V0 results. Moreover, the addition of a small amount of SAN had little influence on the flame retardancy of PC-based composites. With increase in SAN content, the LOI value gradually decreased, while the UL94 rating changed from V0 to V1. When the SAN content was 5% and 8%, the LOI values of PC/SAN$_x$@(CCF+GNP) were decreased by 2.3% and 4.8%, respectively. However, light smoke and no dripping were observed for each sample in the testing process. On the other hand, as RXP content increased, the LOI value of *r*PC/SAN$_5$@(CCF+GNP)$_i$ was clearly improved. The LOI value reached 37.9% when 2.5% of RXP was added in PC/SAN$_5$@(CCF+GNP). Correspondingly, regardless of RXP content, the flame retardant composites achieved V0 rating in the UL94 test, and released light smoke.

Table 4. Effects of SAN and RXP on flame retardancy of PC-based composites.

Sample	LOI (%)	UL94 classes	Smoke	Dripping
PC/SAN$_0$@(CCF+GNP)	31.0	V0	Light	No
PC/SAN$_3$@(CCF+GNP)	31.2	V0	Light	No
PC/SAN$_5$@(CCF+GNP)	30.3	V1	Light	No
PC/SAN$_8$@(CCF+GNP)	29.5	V1	Light	No
*r*PC/SAN$_5$@(CCF+GNP)$_{0.5}$	32.1	V0	Light	No
*r*PC/SAN$_5$@(CCF+GNP)$_{1.5}$	34.9	V0	Light	No
*r*PC/SAN$_5$@(CCF+GNP)$_{2.5}$	37.9	V0	Light	No

Table 5. The mechanical properties of PC-based composites.

Sample	Notched impact strength (kJ m^{-2})	Flexural strength (MPa)	Flexural modulus (MPa)	Tensile strength (MPa)	Elongation at break (%)	Tensile modulus (MPa)
PC/SAN$_0$@(CCF+GNP)	4.8 ± 0.9	111 ± 3	10312 ± 190	97 ± 3	1.54 ± 0.15	9761 ± 61
PC/SAN$_3$@(CCF+GNP)	5.1 ± 0.5	122 ± 3	10473 ± 92	106 ± 3	1.63 ± 0.08	11437 ± 439
PC/SAN$_5$@(CCF+GNP)	5.0 ± 0.3	130 ± 9	10963 ± 159	108 ± 5	1.69 ± 0.08	11743 ± 388
PC/SAN$_8$@(CCF+GNP)	4.9 ± 0.2	138 ± 2	11575 ± 171	118 ± 2	1.68 ± 0.10	11910 ± 49
*r*PC/SAN$_5$@(CCF+GNP)$_{0.5}$	4.5 ± 0.4	133 ± 2	11200 ± 60	113 ± 2	1.67 ± 0.06	12000 ± 423
*r*PC/SAN$_5$@(CCF+GNP)$_{1.5}$	4.6 ± 0.3	144 ± 2	11625 ± 223	120 ± 1	1.69 ± 0.05	12180 ± 58
*r*PC/SAN$_5$@(CCF+GNP)$_{2.5}$	5.2 ± 0.6	139 ± 5	11879 ± 127	118 ± 6	1.73 ± 0.09	12298 ± 141

4.3 Mechanical properties and fractography

The mechanical properties of the PC-based composites with different contents of SAN and RXP are listed in Table 5. With the incorporation of SAN, the notched impact strength and the elongation yield at break of PC/SAN$_x$@(CCF+GNP) varied slightly. However, the flexural and tensile strengths as well as the flexural and tensile moduli of composites increased sequentially. When the SAN content was 5%, the flexural strength and modulus of PC/SAN$_5$@(CCF+GNP) were 130 MPa and 10963 MPa, respectively, which increased by approximately 17.1% and 6.3% compared to those of PC/SAN$_0$@(CCF+GNP); meanwhile, the tensile strength and modulus were 108 MPa and 11743 MPa, which improved by about 11.3% and 20.3%, respectively. SAN could act as rheology modifier and it could have enhanced the matrix/fillers interfacial bonding, reduced the performance defects, and improved the mechanical strength of PC-based composites.

Besides, with increase of RXP content, the flexural and tensile strengths of *r*PC/SAN$_5$@(CCF+GNP)$_i$ increased and then decreased slightly, while the flexural and tensile moduli increased incrementally. In comparison with PC/SAN$_5$@(CCF+GNP), when the RXP content was 2.5%, the flexural strength and modulus of *r*PC/SAN$_5$@(CCF+GNP)$_{2.5}$ were 139 MPa and 11879 MPa, which increased by approximately 6.9% and 8.4%, respectively; and the tensile strength and modulus were 118 MPa and 12298 MPa, which improved by about 9.3% and 4.7%, respectively. That was likely caused by the inter-molecular transesterification reaction between the carbonate group of PC and the phosphate group of RXP, as a result, RXP further improved the compatibility of composite system.

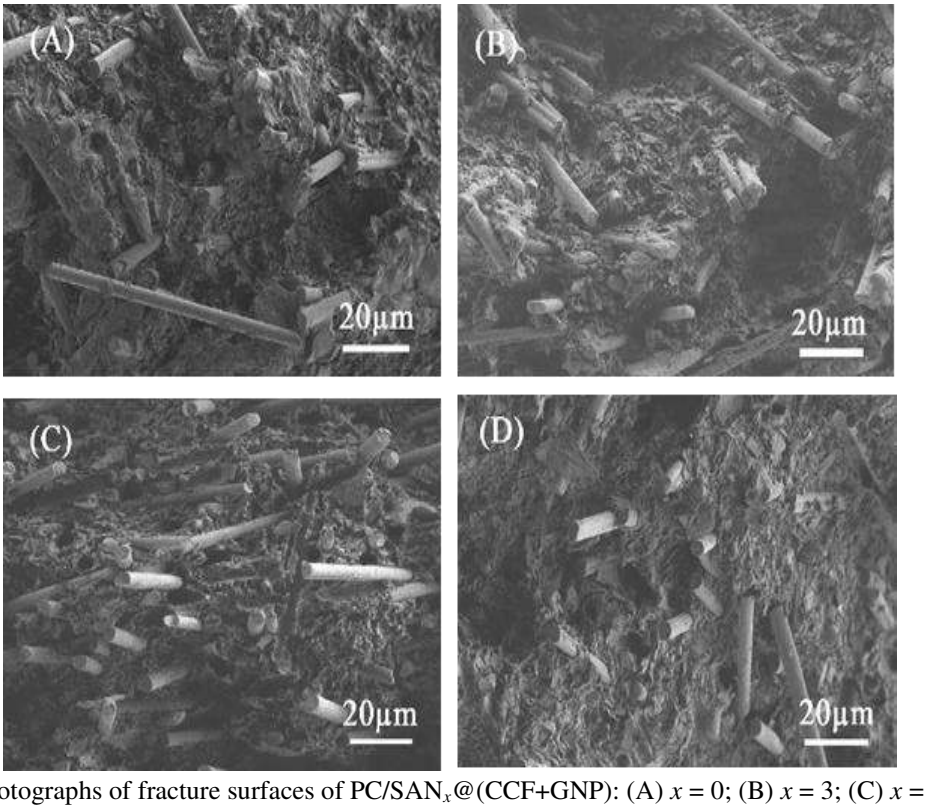

Fig. 7 SEM photographs of fracture surfaces of PC/SAN$_x$@(CCF+GNP): (A) x = 0; (B) x = 3; (C) x = 5; (D) x = 8.

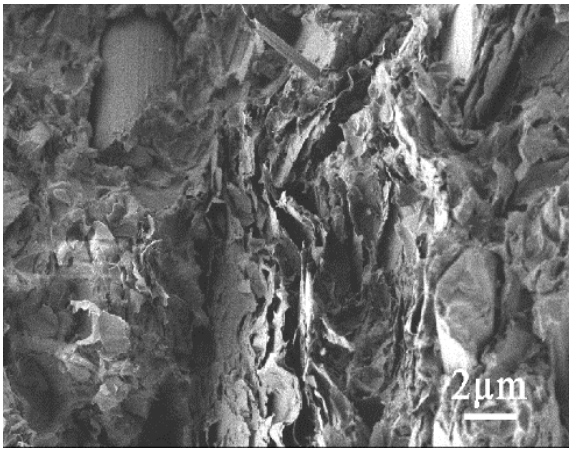

Fig. 8 SEM photograph of fracture surfaces of PC/SAN$_0$@(CCF+GNP) with high magnification.

From the fractographic images of PC/SAN$_x$@(CCF+GNP) composites (Figs. 7 and 8), it could be seen that the short carbon fibers and graphene nanoplatelets dispersed uniformly in matrix. There also existed a number of circular cavities and naked fibers, which formed because of fiber breaking or peeling from matrix under external forces during sample testing. That also confirmed a more rigid composite with more SAN amount had high mechanical strength and modulus. As for *r*PC/SAN$_5$@(CCF+GNP)$_i$, the amount of long naked fibers increased and the surface tended to be apparently uneven (Fig. 7C and Fig. 9). In other words, with increase of RXP content, the total peeling of matrix exacerbated. The interface between PC matrix and hybrid carbon fillers was effectively enhanced. This was also the main reason for composites possessing high strength and modulus.

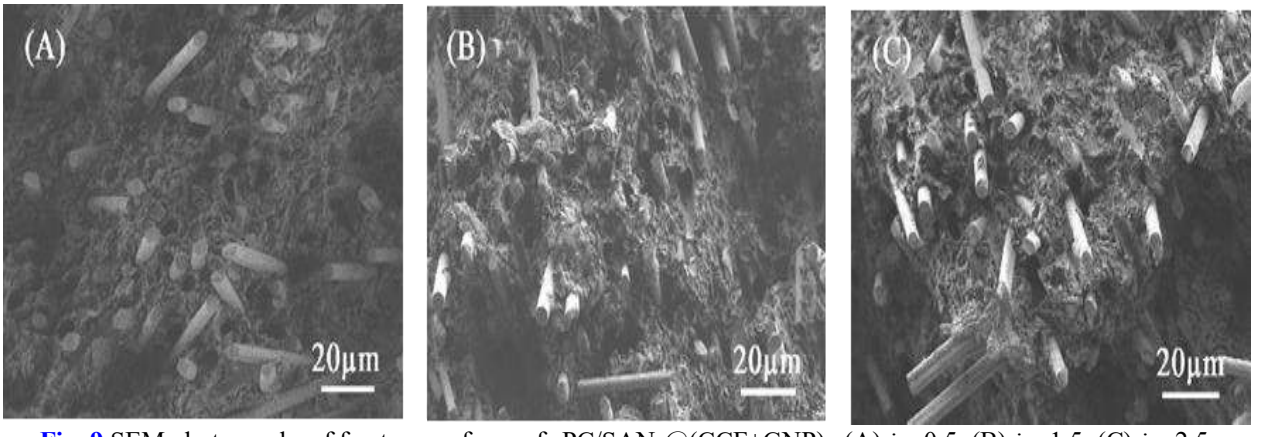

Fig. 9 SEM photographs of fracture surfaces of *r*PC/SAN$_5$@(CCF+GNP)$_i$: (A) i = 0.5; (B) i = 1.5; (C) i = 2.5.

5. Conclusions

In this study, PC-based composites with good flow properties and flame retardancy were prepared by a melt extrusion blending process. In the rheological study, all of PC-based composites basically showed non-Newtonian fluid behaviors in the shear rate of 0.1 s^{-1} to 100 s^{-1}. The apparent viscosity of all PC-based composites decreased obviously with increasing shear rate and temperature. At the same shear rate and temperature, the apparent viscosity of PC/SAN$_x$@(CCF+GNP) slightly increased with SAN content increasing, while that of PC/SAN$_5$@(CCF+GNP)$_i$ decreased a little with RXP content increasing. Through linear fitting and calculation, PC/SAN$_5$@(CCF+GNP) showed higher viscous flow activation energy and greater temperature sensitivity of viscosity than PC/SAN$_0$@(CCF+GNP) and *r*PC/SAN$_5$@(CCF+GNP)$_{1.5}$. While PC/SAN$_0$@(CCF+GNP) also exhibited a strong sensitivity to shearing force compared to *r*PC/SAN$_5$@(CCF+GNP)$_{1.5}$.

Incorporating SAN and RXP in the composites was beneficial for the thermal stability of PC/SAN$_x$@(CCF+GNP) and *r*PC/SAN$_x$@(CCF+GNP)$_i$. The LOI of the PC-based composite with 2.5 % RXP increased to 37.9%, and the flame retardant PC-based composite passed V-0 rating in the UL-94 test. Meanwhile, the flexural and tensile strengths and moduli of PC-based composites also increased as SAN and RXP contents were increased, while the notched impact strength and elongation at break were not impaired. Fractography confirmed that the incorporation of SAN and RXP could effectively enhance the interfacial interactions of PC and hybrid carbon fillers.

Acknowledgements

The authors would like to acknowledge the help of Huining Zhang (A senior engineer at Sinopec Shanghai Research Institute of Petrochemical Technology) for the morphology characterization and the reviewers for the helpful suggestions.

Conflict of interest

There are no conflicts to declare.

Supporting information

Not applicable

References

[1] G. Chabaud, M. Castro, C. Denoual and A. Le Duigou, *Addit. Manuf.*, 2019, **26**, 94-105, doi: 10.1016/j.addma.2019.01.005.

[2] N. T. Kamer, L. T. Drzal, A. Lee and P. Askeland, *Polymer*, 2017, **111**, 36-47, doi: 10.1016/j.polymer.2017.01.009.

[3] H. Oliver-Ortega, F. Julian, F. X. Espinach, Q. Tarrés, M. Ardanuy and P. Mutjé, *J. Clean. Prod.*, 2019, **226**, 64-73, doi: 10.1016/j.jclepro.2019.04.047.
[4] T. T. Yao, G. P. Wu and C. Song, *Compos. Sci. Technol.*, 2017, **149**, 108-115, doi: 10.1016/j.compscitech.2017.06.017.
[5] F. Lambiase, S. Genna, C. Leone and A. Paoletti, *Opt. Laser Technol.*, 2017, **94**, 45-58, doi: 10.1016/j.optlastec.2017.03.006.
[6] S. Fu, B. Lauke and Y. Mai, Science and Engineering of Short Fibre-Reinforced Polymer Composites (Second Edition), Woodhead: Cambridge, 2019, 213-240, doi: 10.1016/B978-0-08-102623-6.00008-1.
[7] Z. K. Zhao, S. S. Du, F. Li, H. M. Xiao, Y.Q. Li, W. G. Zhang, N. Hu and S. Y. Fu, *Compos. Commun.*, 2018, **8**, 1-6, doi: 10.1016/j.coco.2018.02.001.
[8] F. Li, Y. Hua, C. B. Qu, H. M. Xiao and S. Y. Fu, *Compos. Part A*, 2016, **89**, 47-55, doi: 10.1016/j.compositesa.2016.02.016.
[9] L. Leveuf, Y. Marco, V. Le Saux, L. Navrátil, S. Leclercq, and J. Olhagaray, *Polym. Test.*, 2018, **68**, 19-26, doi: 10.1016/j.polymertesting.2018.03.045.
[10] I. L. Ngo, C. Byon, *Sci. Adv. Mater.*, 2016, **8**, 257-266, doi: 10.1166/sam.2016.2476.
[11] C. Liu, M. Chen, W. Yu and Y. He, *ES Energy Environ.*, 2018, **2**, 31-42, doi: 10.30919/esee8c191.
[12] L. Tzounis, T. Gärtner, M. Liebscher, P. Pötschke, M. Stamm, B. Voit and G. Heinrich, *Polymer*, 2014, **55**, 5381-5388, doi: 10.1016/j.polymer.2014.08.048.
[13] M. Liebscher, T. Gärtner, L. Tzounis, M. Mičušík, P. Pötschke, M. Stamm, G. Heinrich and B. Voit, *Compos. Sci. Technol.*, 2014, **101**, 133-138, doi: 10.1016/j.compscitech.2014.07.009.
[14] F. Y. Castillo, R. Socher, B. Krause, R. Headrick, B. P. Grady, R. Prada-Silvy and P. Pötschke, *Polymer*, 2011, **52**, 3835-3845, doi: 10.1016/j.polymer.2011.06.018.
[15] G. Gedler, M. Antunes, T. Borca-Tasciuc, J. I. Velasco and R. Ozisik, *Eur. Polym. J.*, 2016, **75**, 190-199, doi: 10.1016/j.eurpolymj.2015.12.018.
[16] H. S. Kim, J. H. Kim, C. M. Yang, and S. Y. Kim, *J. Alloys. Compound.*, 2017, **690**, 274-280, doi: 10.1016/j.jallcom.2016.08.141.
[17] C. Yang, X. H. Yin, X. P. Li, Z. H. Zhang, J. W. Kan and G. M. Cheng, *Appl. Therm. Eng.*, 2016, **100**, 1207-1218, doi: 10.1016/j.applthermaleng.2016.03.002.
[18]. X. Jin, J. Wang, L. Dai, W. Wang and H. Wu, *Compos. Sci. Technol.*, 2019, **184**, 107862, doi: 10.1016/j.compscitech.2019.107862.
[19] B. Wen and X. Zheng, *Compos. Sci. Technol.*, 2019, **174**, 68-75, doi: 10.1016/j.compscitech.2019.02.017.
[20] S. Zhou, Y. Chen, H. Zou and M. Liang, *Thermochim Acta*, 2013, **566**, 84-91, doi: 10.1016/j.tca.2013.05.027.
[21] T. M. Baek, P. S. Shin, J. H. Kim, H. S. Park, K. L. DeVries and J. M. Park, *Polym. Test.*, 2020, **81**, 106247, doi: 10.1016/j.polymertesting.2019.106247.
[22] N. Bagotia, V. Choudhary and D. K. Sharma, *Compos. Part B*, 2019, **159**, 378-388, doi: 10.1016/j.compositesb.2018.10.009.
[23] C. Xiao, X. Leng, X. Zhang, K. Zheng and X. Tian, *Compos. Part A*, 2018, **110**, 133-141, doi: 10.1016/j.compositesa.2018.03.030.
[24] C. M. Gómez, M. Culebras, A. Cantarero, B. Redondo-Foj, P. Ortiz-Serna, M. Carsí and M. J. Sanchis, *Appl. Surf. Sci.*, 2013, **275**, 295-302, doi: 10.1016/j.apsusc.2012.12.108.
[25] N. Bagotia, V. Choudhary and D. K. Sharma, *Compos. Part B*, 2017, **124**, 101-110, doi: 10.1016/j.compositesb.2017.05.037.
[26] Z. Yu, Y. Bai, Y. Li and W. Wang, *Petrochem. Technol.*, 2018, **47**, 170-175, doi: 10.3969/j.issn.1000-8144.2018.02.010.
[27] C. Ozkan, N. G. Karsli, A. Aytac and V. Deniz, *Compos. Part B*, 2014, **62**, 230-235, doi: 10.1016/j.compositesb.2014.03.002.
[28] Z. Yu, Y. Bai, Y. Li, W. Wang and J. H. Wang, *J. Mater. Sci. Chem. Eng.*, 2018, **6**, 81-89, doi: 10.4236/msce.2018.67009.
[29] Z. Yu, Y. Bai, Y. Li, X. Wang, W. Wang and J. Liu, *Polym. Int.*, 2018, **67**, 1137-1144, doi: 10.1002/pi.5628.
[30] S. Sharma, R. Chandra, P. Kumar and N. Kumar, *C. R. Mecanique*, 2015, **343**, 371-396, doi: 10.1016/j.crme.2015.03.002.
[31] M. C. Despinasse, B. Schartel, *Polym. Degrad. Stab.*, 2012, **97**, 2571-2580, doi: 10.1016/j.polymdegradstab.2012.07.005.
[32] M. C. Despinasse, B. Schartel, *Thermochim Acta*, 2013, **563**, 51-61, doi: 10.1016/j.tca.2013.04.006.
[33] N. Wu, S. Lang, *Polym. Degrad. Stab.*, 2016, **123**, 26-35, doi: 10.1016/j.polymdegradstab.2015.11.007.
[34] J. Zhang, *Procedia Eng.*, 2016, **135**, 83-89, doi: 10.1016/j.proeng.2016.01.083.
[35] M. J. Shirkavand, H. Azizi, I. Ghasemi, M. Karrabi and R. Rashedi, *Iran Polym. J.*, 2015, **24**, 953-96, doi: 10.1007/s13726-015-0383-7.
[36] C. Lohr, S. Dieterle, A. Menrath, K. A. Weidenmann and P. Elsner, *Polym. Test.*, 2018, **71**, 27-31, doi: 10.1016/j.polymertesting.2018.08.015.
[37] F. Baldi, A. Franceschini and F. Bignotti, *Polym. Test.*, 2011, **30**, 765-772, doi: 10.1016/j.polymertesting.2011.07.002.
[38] A. M. Jordan, P. Lee, C. Thurber and C. W. Macosko, *Ind. Eng. Chem. Res.*, 2018, **57**, 14106-14113, doi: 10.1021/acs.iecr.8b03674.
[39] Q. Wu and J. Wu, *Polymer rheology*, Beijing Higher Education: Beijing, 2002, 1-5, doi: 10.1016/B978-0-323-24273-8.00005-8.
[40] J. Innes and A. Innes, *Plast. Add. Compound.*, 2006, **8**, 26-29, doi: 10.1016/S1464-391X(06)70523-2.

Author information

Zhixing Yu *is a senior engineer at Sinopec Shanghai Research Institute of Petrochemical Technology. He has published 25 papers and received 25 granted Chinese patents. His scientific research concentrates on synthesis, processing modification and application of functional composite materials, including heat transfer, laser activation and dielectric*

materials. He received his PhD in Materials Science and Engineering from Dalian University of Technology, China.

Yu Bai *is a senior engineer and he focuses on research and development of modified polymer materials in Sinopec Shanghai Research Institute of Petrochemical Technology. He received his PhD in Polymer Chemistry and Physics in Peking University in 2008.*

James H. Wang *is a Sinopec Corporate Fellow and a Chief Expert at Sinopec Shanghai Research Institute of Petrochemical Technology. He received 400 granted patents including over 120 granted U.S. patents. He was elected as a Fellow of American Institute for Medical and Biological Engineering in 2019, a Fellow of American Chemical Society (ACS) in 2017, a Fellow of Polymer Chemistry in 2014, and a Fellow of Polymeric Materials Science and Engineering in 2013. He received the "Industrial Polymer Scientist Award" from ACS Division of Polymer Chemistry in 2020. His research focuses on functional polymers, sustainable polymers, polymer modification and processing technologies. He received his MS in Sustainable Biomaterials from Virginia Tech and PhD in Macromolecular Science from Case Western Reserve University.*

Yingcheng Li *is a senior expert at Sinopec, deputy chief engineer of Sinopec Shanghai Research Institute of Petrochemical Technology. His research focuses on the development of new surfactants for enhanced oil recovery and new synthetic materials. He holds a PhD degree in Physical Chemistry from Fudan University, China.*

Publisher's Note: Engineered Science Publisher remains neutral with regard to jurisdictional claims in published maps and institutional affiliations.